Theor Chem Acc (2010) 125:45–55
DOI 10.1007/s00214-009-0657-2

REGULAR ARTICLE

Theoretical investigation on mechanism for OH-initiated oxidation of CH_2=C(CH_3)CH_2OH

Weichao Zhang · Benni Du · Changjun Feng

Received: 2 August 2009 / Accepted: 6 October 2009 / Published online: 29 October 2009

Abstract The mechanism of the gas-phase reaction OH with CH_2=C(CH_3)CH_2OH (2-methyl-2-propen-1-ol) has been elucidated using high-level ab initio method, i.e., CCSD(T)/6-311++g(d,p)//MP2(full)/6-311++g(d,p). Various possible H-abstraction and addition–elimination pathways are identified. The calculations indicate that the addition–elimination mechanism dominates the OH+MPO221 reaction. The addition reactions between OH radicals and CH_2=C(CH_3)CH_2OH begin with the barrierless formation of a pre-reactive complex in the entrance channel, and subsequently the CH_2(OH)C(CH_3)CH_2OH (IM1) and the CH_2C(OH)(CH_3)CH_2OH (IM2) are formed by OH radicals' electrophilic additions to the double bond. IM1 can easily rearrange to IM2 via a 1,2-OH migration. Subsequently, rearrangement of IM2 to form (CH_3)$_2$C(OH)CH_2O (IM11) followed by dissociation to HCHO + (CH_3)$_2$COH (P21) is the most favorable pathway. The decomposition of IM2 to CH_2OH + CH_2=C(OH)CH_3 (P16) is the secondary pathway. The other pathways are not expected to play any important role in forming final products.

Keywords OH radicals · CH_2=C(CH_3)CH_2OH · Reaction mechanism · CCSD(T) · MP2

1 Introduction

Unsaturated alcohols are a kind of volatile organic compounds (VOCs) released into the atmosphere by various sources (e.g. plastic industries, polymer synthesis, several varieties of pine, and other types of vegetation, etc.) and act as primary pollutants [1, 2]. These compounds are known to play an important role in tropospheric chemistry [3].

Unsaturated alcohols could be chemically removed from the troposphere by reaction with different reactive species like radicals and ozone, by wet and dry deposition. However, the reactions with hydroxyl radicals (OH) and ozone during the day and with NO_3 radicals at night are believed to be the dominant degradation processes for unsaturated alcohols.

Experimentally, the reactions of unsaturated alcohols with OH radicals [2, 4–8], NO_3 radicals [9, 10], Cl atom[11, 12], and O_3 [6, 13, 14] have been the most widely investigated and gas-phase rate constants have been determined in several works. However, research about mechanistic information or product determination is scarce.

There is only single study of the CH_2=C(CH_3)CH_2OH (denoted as MPO221) reaction with OH radicals. Recently, Cometto et al. used a conventional relative rate method and the pulsed laser photolysis-laser induced fluorescence technique to measure the rate constants of OH+MPO221 over the temperature range of 263–371 K [2]. They observed a negative temperature dependence for this reaction and reported the Arrhenius expression: $k = (10 \pm 1) \times 10^{-12}$

Electronic supplementary material The online version of this article (doi:10.1007/s00214-009-0657-2) contains supplementary material, which is available to authorized users.

W. Zhang (✉) · B. Du
College of Chemistry and Chemical Engineering,
Xuzhou Normal University, 221116 Xuzhou, Jiangsu,
People's Republic of China
e-mail: zwc@xznu.edu.cn

C. Feng
College of Chemistry and Chemical Engineering,
Xuzhou Institute of Technology, 221008 Xuzhou, Jiangsu,
People's Republic of China

exp((652 ± 27)/T) cm^3 $molecule^{-1}$ s^{-1}, and the rate constant at 298 K is (9.3 ± 0.2) × 10^{-11} cm^3 $molecule^{-1}$ s^{-1}.

As a supplement to the experiments, we present here an extensive theoretical study on the reaction of OH radicals with MPO221. To our knowledge, this work provides the first theoretical study using the high-level quantum chemical method. The main aim of the present study is to elucidate the reaction mechanism and to enrich data of this kind of reactions from a theoretical point of view.

2 Theoretical approach

Ab initio molecular orbital calculations were carried out using the Gaussian 03 program [15]. The geometrical structures of all the reactants, intermediates, transition states, and the products were optimized using Møller-Plesset correlation energy correction truncated at second-order (MP2) theory [16, 17] (including all the electrons in the correlation treatment) with Pople's split-valence 6-311++G(d,p) basis set [18, 19]. Accordingly, we denoted our MP2 calculations by MP2(full)/6-311++G(d,p).

The optimized equilibrium structures (local minima and first-order transition states) were confirmed with calculations of vibrational frequencies at the same level of theory. The reactants, intermediates, and products had no imaginary frequencies, whereas the transition states possessed only one imaginary frequency. The correction for zero-point energy (ZPE) was also considered at the level MP2(full)/6-311++G(d,p). Frequency calculations on the optimized structures were also used to generate the zero-point corrections to be added to the potential energy in order to calculate the zero-point-corrected energy.

In addition, intrinsic reaction coordinate (IRC) calculations with the Gonzalez–Schlegel second-order method [20, 21] were performed at the same level of theory to confirm that the transition states really connect to appropriate reactants and products along the reaction path. The step size used for the IRC calculations was 0.1 $(amu)^{1/2}$ bohr [22].

To further correct for electron correlation, single-point energy calculations were performed uniformly by means of coupled cluster method with single, double, and perturbative triple configurations (CCSD(T)) [23] with the 6-311++G(d,p) basis set using the geometry optimized at MP2(full)/6-311++G(d,p) level. The highest level of theory attained in this work can thus be denoted CCSD(T)/6-311++G(d,p)//MP2(full)/6-311 +G(d,p). Addition of zero-point energy correction (ZPE) to the single-point energy, i.e., CCSD(T)/6-311++G(d,p)//MP2(full)/6-311++G(d,p) + ZPE, was chosen for the following discussion, unless mentioned otherwise.

3 Results and discussion

Figures 1, 2 and 3 show the predicted geometric parameters of the initial reactants, intermediates (IMs), transition states (TSs), and products from MP2(full)/6-311++G(d,p) calculations. The calculated ZPE corrections and relative energies of all the stationary points involved in the OH+MPO221 reaction are listed in Table 1. The calculated total energies of the various species involved in the title reaction are given in Table S1 in Supporting information. The profile of the potential energy surfaces for the reaction of OH radicals with MPO221 at the CCSD(T)/6-311++G(d,p)//MP2(full)/6-311++G(d,p)+ZPE level are presented in Figs. 4, 5 and 6, respectively.

3.1 Entrance channels

There are two possible reaction patterns for the initial reaction of OH radicals with MPO221, i.e., direct H-abstraction and OH-addition mechanisms. As seen in Fig. 4, five direct H-abstraction channels have been identified. The OH radicals may abstract H atoms in methylene group (=CH_2) via TS1 and TS2, respectively. The corresponding products are CH=C(CH_3)CH_2OH (P1)+H_2O and CH=C(CH_3)CH_2OH (P2)+H_2O. Both transition states have a high relative energy of about 30–38 kJ mol^{-1} above the original reactants. The OH radicals can also abstract H atom in methyl group (–CH_3) to produce CH_2=C(CH_2)CH_2OH (P3)+H_2O via TS3 with a barrier height of 25.83 kJ mol^{-1}. From Fig. 2, it can be seen that P3 has an allyl radical structure. The MP2 wave function is not appropriate to describe delocalized radicals. TS3 possesses the same question like mentioned above. In these cases, the multiconfiguration CASSCF(5,5) method [24, 25], in conjunction with the 6-311G(d,p) basis set, is employed to re-optimize geometries. The relative energies of P3 and TS3 are then re-calculated using the CCSD(T)/6-311++G(d,p) level of theory. The fourth H-abstraction channel is that OH radicals abstracts H atom in methylene group (–CH_2–) to form CH_2=C(CH_3)CHOH (P4)+H_2O via TS4, facing a low barrier height of 3.53 kJ mol^{-1}. On the last H-abstraction pathway, OH radicals abstracts H atom in hydroxy group (–OH) to produce CH_2=C(CH_3)CH_2O (P5)+H_2O via TS5. The barrier height for this step is 15.49 kJ mol^{-1}. It can be seen from Fig. 4 that P1 + H_2O, P2 + H_2O, P3 + H_2O, P4 + H_2O and P5 + H_2O sit below the initial reactants by 9.73, 9.00, 104.63, 134.28, and 45.36 kJ mol^{-1}, respectively. Evidently, only the fourth channel is of interest. It is both thermodynamically and kinetically much more competitive than the other channels.

There are two steps in the process of OH radicals adding to the double bond: first, the reactants OH and MPO221 form a pre-reactive complex (denoted as PC) with

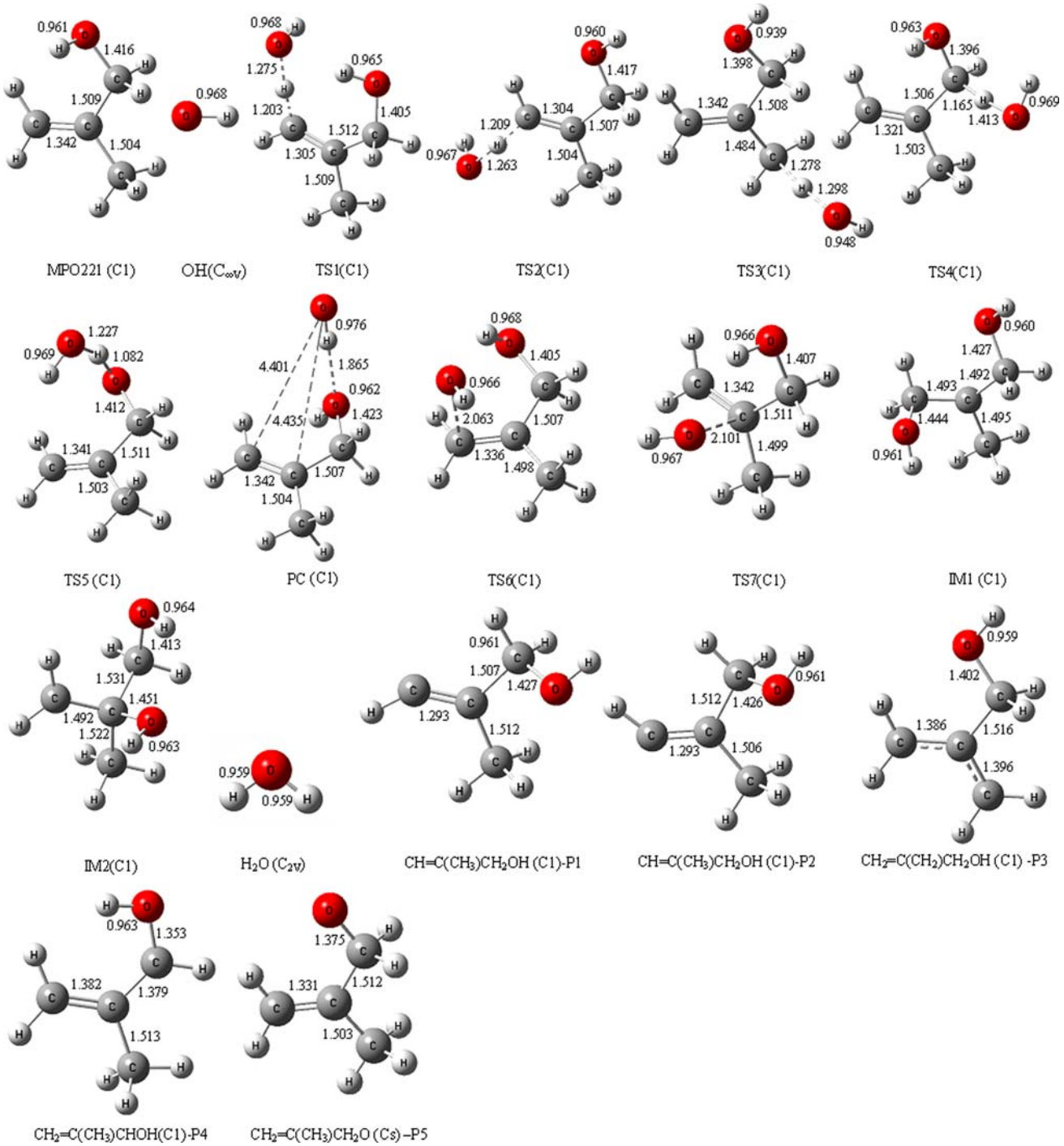

Fig. 1 MP2(full)/6-311++G(d,p) optimized geometries for the reactant, intermediates, transition states, and products involved in the initial reaction of OH radicals with MPO221. Distances are in angstroms

the two O–C bond lengths of 4.401 Å and 4.435 Å, respectively; in the second step, OH radicals attack the unsaturated carbon atom forming a HO–C bond giving an intermediate. When O atom of OH radicals adds to the terminal unsaturated carbon atom of MPO221, the intermediate $CH_2(OH)C(CH_3)CH_2CH_2OH$ (IM1) is formed via TS6. IM1 is 98.61 kJ mol^{-1} lower in energy than the initial reactants. On the other hand, O atom of OH radicals can also attack another unsaturated carbon atom of MPO221 via TS7 forming the intermediate $CH_2C(OH)(CH_3)CH_2CH_2OH$ (IM2), which lies 123.99 kJ mol^{-1} below the initial reactants. The barrier heights for TS6 and TS7 are 16.96 and 11.01 kJ mol^{-1}, respectively. Also, IM2 is calculated to be 25.38 kJ mol^{-1} more stable than IM1.

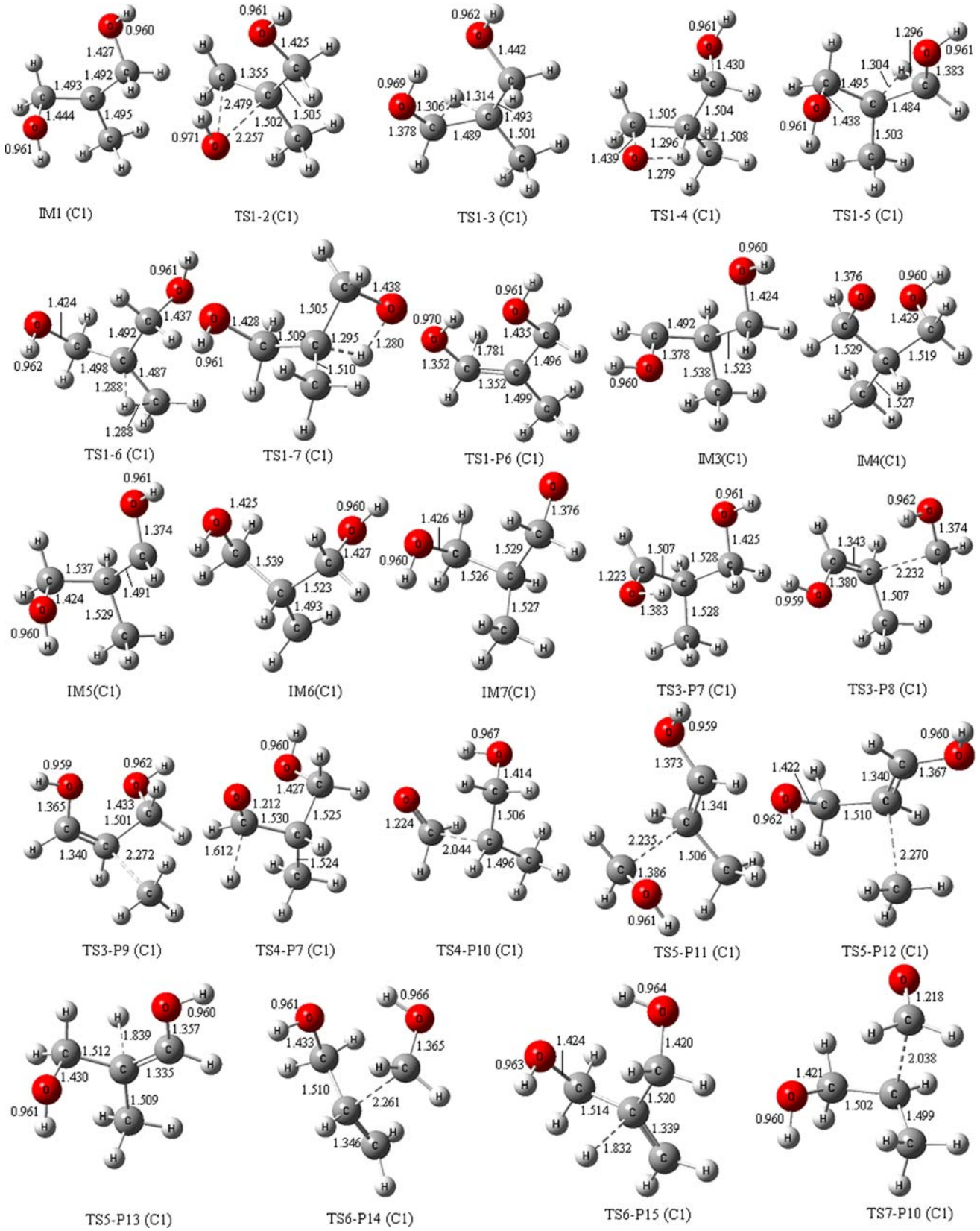

Fig. 2 MP2(full)/6-311++G(d,p) optimized geometries for the intermediates, transition states, and products involved in the unimolecular reaction of the adduct $CH_2(OH)C(CH_3)CH_2OH$ (IM1). Distances are in angstroms. The geometries of TS3 and P3 are optimized at the CSASCF(5,5)/6-311G(d,p) level of theory

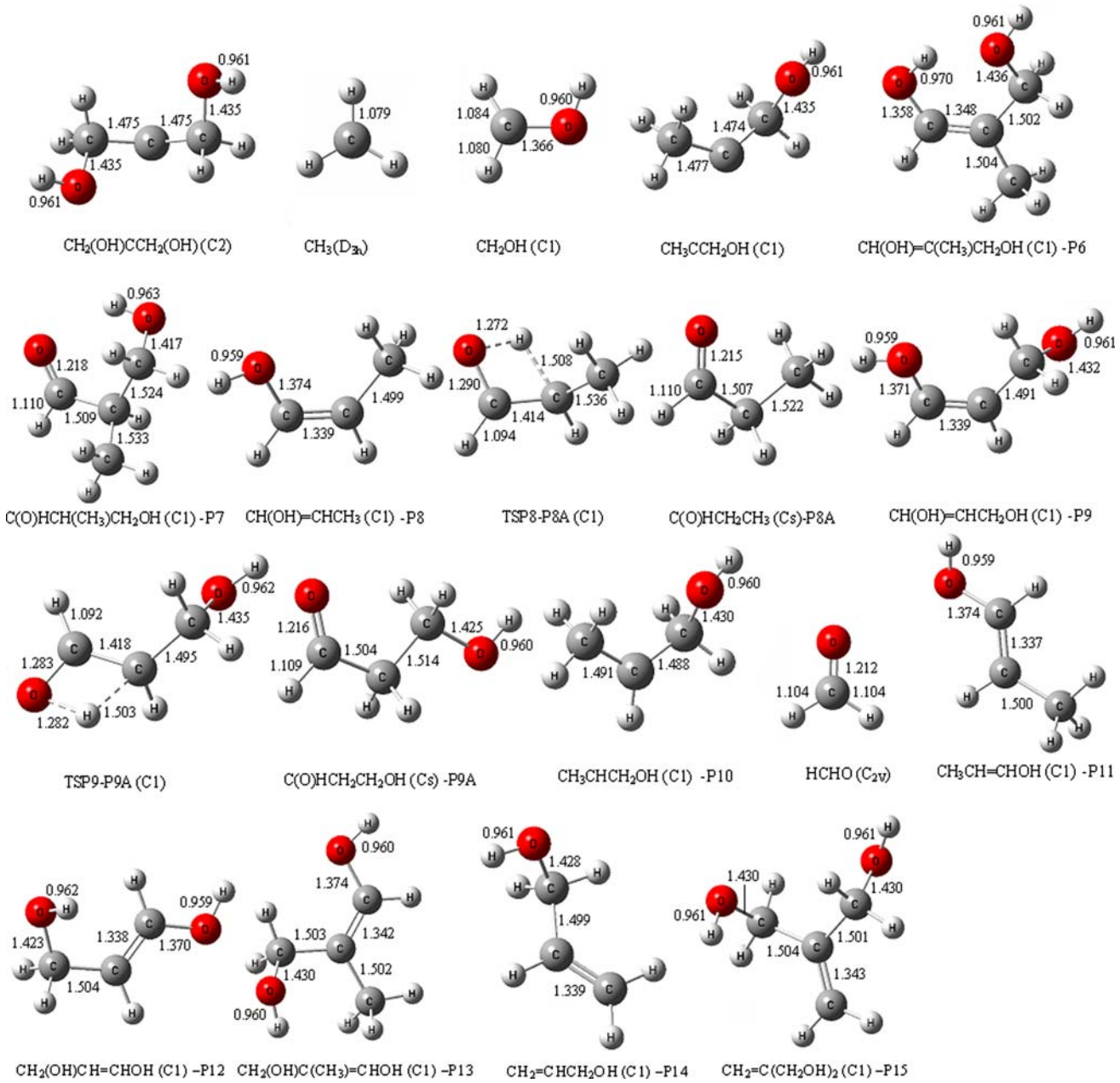

Fig. 2 continued

Therefore, the formation of IM2 is both kinetically and thermodynamically more favored than the formation of IM1. This is consistent with the fact that the HOMO–LUMO (HL) gap of IM2 is higher than that of IM1. The HL gap of an adduct will play an important role in determining its stabilization [26]. Using the HOMO and LUMO energies calculated at the MP2(full)/6-311++G(d,p) level, the HL gaps are predicted to be 0.38121 and 0.41280 a.u. for IM1 and IM2, respectively. The higher HL gap of IM2 indicates that IM2 is more stable than IM1.

Compared with the H-abstraction transition states TS1, TS2, TS3, TS4, and TS5, the addition transition states TS6 and TS7 have negative relative energies of 5.19, and 11.14 kJ mol^{-1}, respectively. It is clear that the additions are energetically much more favorable than the H-abstractions. Among the H-abstraction pathways, only the H-abstraction channel OH + MPO221 → P4 + H_2O may play an important role at higher temperature.

3.2 The unimolecular reactions of IM1

As seen in Fig. 5, there are many possible reaction pathways starting from IM1. Three types of reaction mechanisms have been found, i.e., dissociation mechanisms,

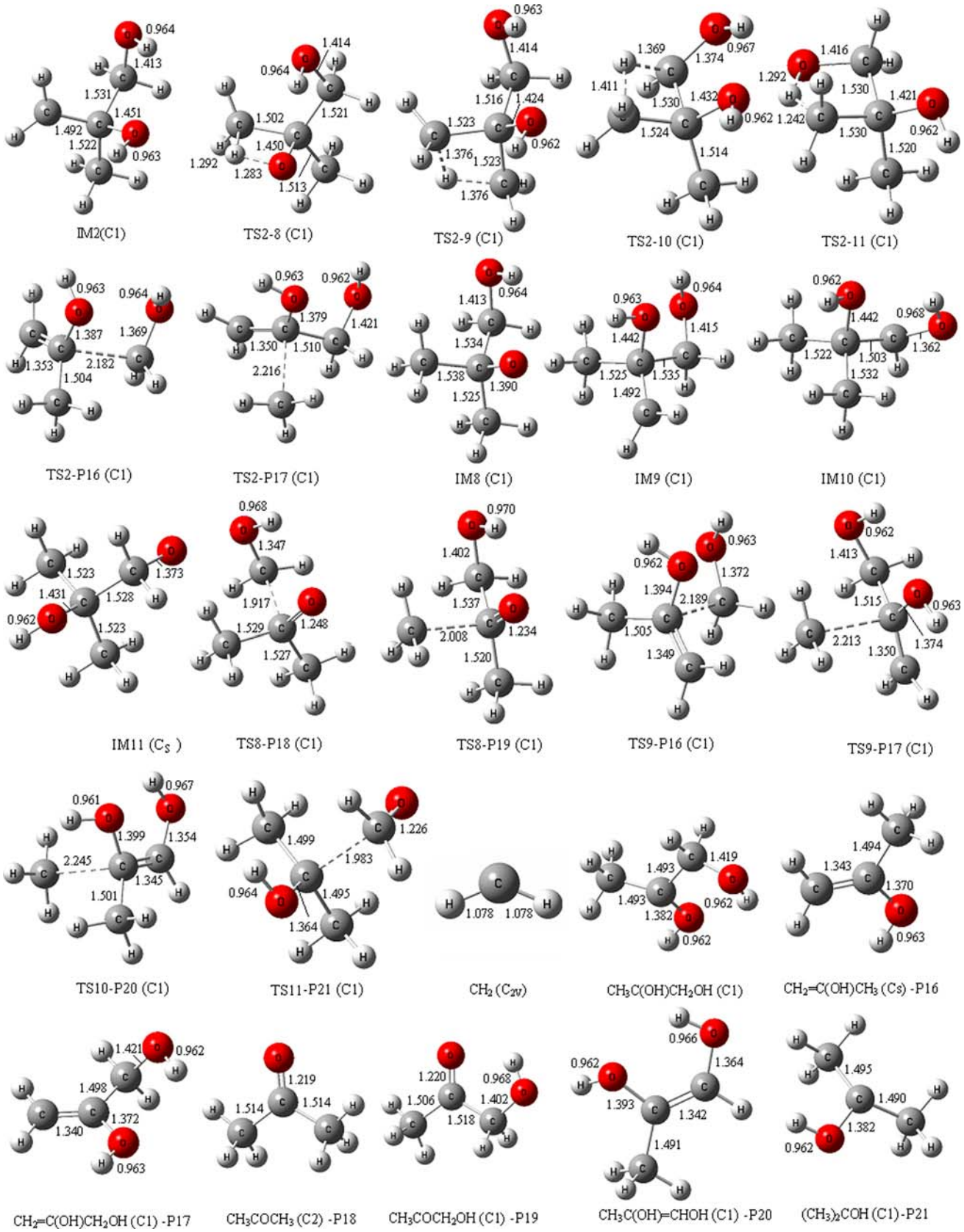

Fig. 3 MP2(full)/6-311++G(d,p) optimized geometries for the intermediates, transition states and products involved in the unimolecular reaction of the adduct $CH_2C(OH)(CH_3)CH_2OH$ (IM2). Distances are in angstroms

Table 1 Calculated relative energy for various species in the OH+MPO221 reaction using CCSD(T)/6-311++G(d,p)//MP2(full)/6-311++G(d,p) level of theory

Species	ZPE[a]	ΔE[b]
OH+MPO221	0.123049	0.00
PC	0.125968	−22.15
TS1	0.122476	30.73
TS2	0.122023	38.03
TS3	0.125485[c]	25.83
TS4	0.123475	3.53
TS5	0.120619	15.49
TS6	0.128392	−5.19
TS7	0.127723	−11.14
TS1-2	0.123688	−13.42
TS1-3	0.126107	73.88
TS1-4	0.126132	34.89
TS1-5	0.125903	78.11
TS1-6	0.125939	72.04
TS1-7	0.126411	36.56
TS1-P6	0.123203	36.94
IM1	0.129901	−98.61
IM2	0.128195	−123.99
IM3	0.129973	−110.01
IM4	0.129995	−82.30
IM5	0.130534	−112.62
IM6	0.129513	−88.96
IM7	0.130154	−78.72
TS3-P7	0.121808	38.13
TS3-P8	0.126313	13.41
TS3-P9	0.125377	31.67
TS4-P7	0.122090	16.79
TS4-P10	0.128273	−23.63
TS5-P11	0.126248	18.68
TS5-P12	0.125593	28.37
TS5-P13	0.122819	51.40
TS6-P14	0.12801	25.94
TS6-P15	0.123992	66.17
TS7-P10	0.127081	−12.82
TS2-8	0.125395	7.69
TS2-9	0.123952	52.13
TS2-10	0.123972	37.56
TS2-11	0.124984	−18.72
TS2-P16	0.126664	2.13
TS2-P17	0.125282	22.50
IM8	0.130171	−108.82
IM9	0.128418	−123.95
IM10	0.129744	−147.42
IM11	0.127683	−110.70
TS8-P18	0.127796	−66.16
TS8-P19	0.126992	−43.43
TS9-P16	0.126502	3.45
TS9-P17	0.125291	22.40
TS10-P20	0.125336	−1.34
TS11-P21	0.127413	−70.48
P1 + H_2O	0.124031	−9.73
P2 + H_2O	0.124002	−9.00
P3 + H_2O	0.125242[c]	−94.33
P4 + H_2O	0.122075	−134.28
P5 + H_2O	0.122675	−45.36
CH_2OH + CH_3CCH_2OH(T)	0.121732	277.06
CH_3 + $CH_2(OH)CCH_2OH$(T)	0.119428	293.20
H + $CH(OH)=C(CH_3)CH_2OH$ (P6)	0.120313	14.15
H + $C(O)HCH(CH_3)CH_2OH$ (P7)	0.119896	−28.03
CH_2OH + $CH(OH)=CHCH_3$ (P8)	0.123526	−24.91
CH_2OH + TSP8-P8A	0.118379	233.92
CH_2OH + $C(O)HCH_2CH_3$ (P8A)	0.123685	−73.16
CH_3 + $CH(OH)=CHCH_2OH$ (P9)	0.121142	−11.48
CH_3 + TSP9-P9A	0.115141	220.55
CH_3 + $C(O)HCH_2CH_2OH$ (P9A)	0.120674	−64.29
HCHO + CH_3CHCH_2OH (P10)	0.122120	−38.97
CH_2OH + $CH_3CH=CHOH$ (P11)	0.123479	−22.13
CH_3 + $CH_2(OH)CH=CHOH$ (P12)	0.120985	−10.41
H + $CH_2(OH)C(CH_3)=CHOH$ (P13)	0.119380	28.13
CH_2OH + $CH_2=CHCH_2OH$ (P14)	0.124017	−1.08
H + $CH_2=C(CH_2OH)_2$ (P15)	0.119989	40.51
CH_2(T) + $CH_3C(OH)CH_2OH$	0.119387	259.20
CH_2OH + $CH_2=C(OH)CH_3$ (P16)	0.123077	−45.04
CH_3 + $CH_2=C(OH)CH_2OH$ (P17)	0.121091	−32.96
CH_2OH + $CH_3C(O)CH_3$ (P18)	0.122808	−100.59
CH_3 + $CH_3C(O)CH_2OH$ (P19)	0.120394	−95.48
CH_3 + $CH_3C(OH)=CHOH$ (P20)	0.120979	−44.50
HCHO + $(CH_3)_2COH$ (P21)	0.123027	−79.00

[a] ZPE (Hartrees) are calculated at the MP2(full)/6-311++G(d,p) level of theory

[b] Relative energies are in kJ mol^{-1}

[c] ZPE of TS3 and P3 are calculated at the CSASCF(5,5)/6-311G(d,p) level of theory

barrierless dissociation mechanisms, and isomerization/dissociation mechanisms.

As can be seen from Fig. 5, IM1 can dissociate to H + $CH(OH)=C(CH_3)CH_2OH$ (P6) via the C–H cleavage transition state TS1-6 overcoming a barrier of 135.55 kJ mol^{-1}. IM1 can directly decompose into CH_2OH + CH_3CCH_2OH and CH_3 + $CH_2(OH)CCH_2OH$ without the corresponding transition states detected. The CH_2OH + CH_3CCH_2OH and CH_3 + $CH_2(OH)CCH_2OH$ dissociation fragments lie 375.67 and 391.81 kJ mol^{-1} above IM1.

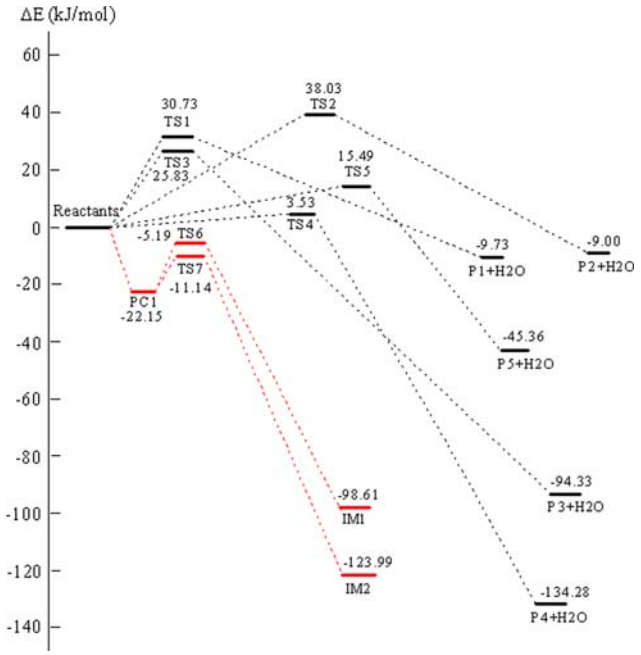

Fig. 4 Profile of the doublet potential energy surface for the initial reaction of OH radicals with CH_2=C(CH_3)CH_2OH at the CCSD(T)/6-311++G(d,p)//MP2(full)/6-311++G(d,p) + ZPE level. Major pathways are indicated in *red*

Thus, the two dissociation channels are energetically less favourable.

There are six isomerization channels from IM1 leading to IM2, IM3, IM4, IM5, IM6, and IM7. Then, these isomers can undergo further changes to form the corresponding products.

The first pathway is that IM1 can isomerize to IM2 via TS1-2 by a 1,2-OH migration. This step is characterized by a barrier height of 85.19 kJ mol^{-1}. From Fig. 5, it can be seen that TS1-2 lies 13.42 kJ mol^{-1} below the initial reactants. Evidently, this isomerization channel is feasible kinetically. It should be mentioned that TS1-2 could not be located using MP2 method. At the MP2(full)/6-31G(d) level, the optimization of TS1-2 always converges to TS6 or TS7. Improving the levels of theory employed cannot avoid this problem. When the geometry of TS1-2 is significantly different from that of TS6 or TS7, the calculation cannot be performed completely. We have detected the value of S^2 for TS1-2 to evaluate if spin contamination can influence the optimization. The value of S^2 is 0.886 after annihilation, where 0.750 is the correct value. Therefore, the geometry of TS1-2 cannot be calculated at the MP2 method may be due to high spin contamination. The geometry parameters of TS1-2 shown in Fig. 2 are characterized using B3LYP method with 6-311++G(d,p) basis set.

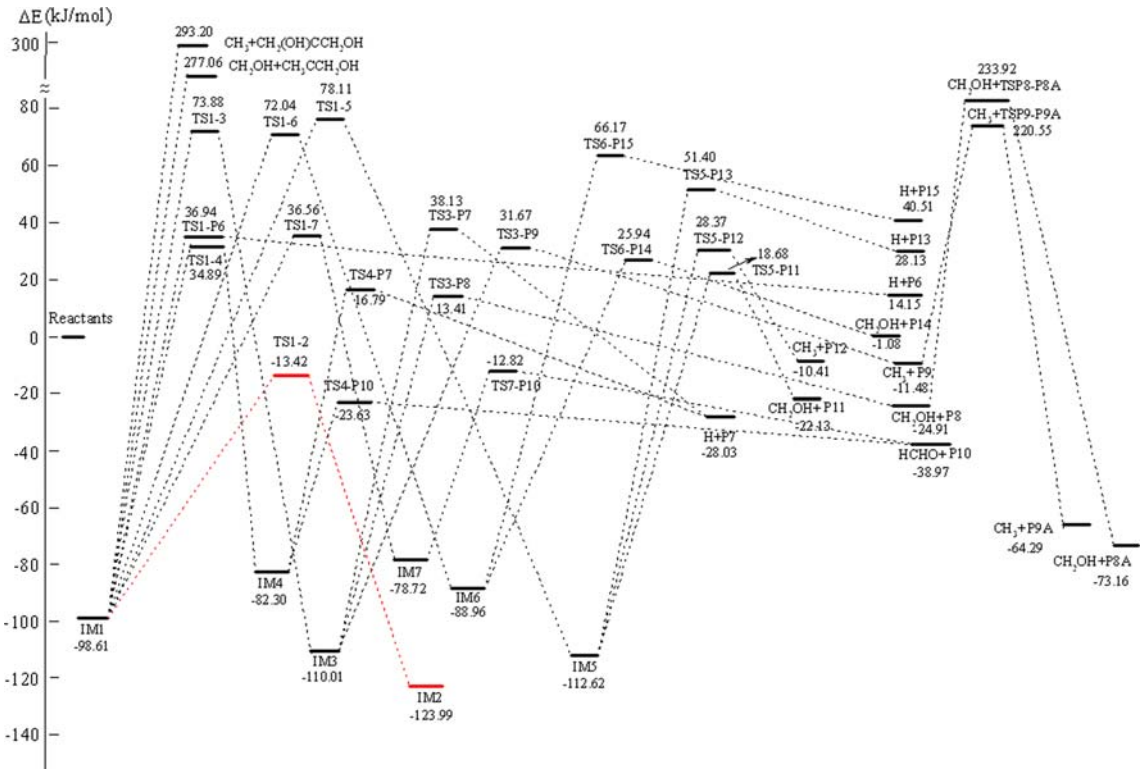

Fig. 5 Profile of the doublet potential energy surface starting from the unimolecular reaction of CH_2(OH)C(CH_3)CH_2OH (IM1) at the CCSD(T)/6-311++G(d,p)//MP2(full)/6-311++G(d,p) + ZPE level. Major pathways are indicated in *red*

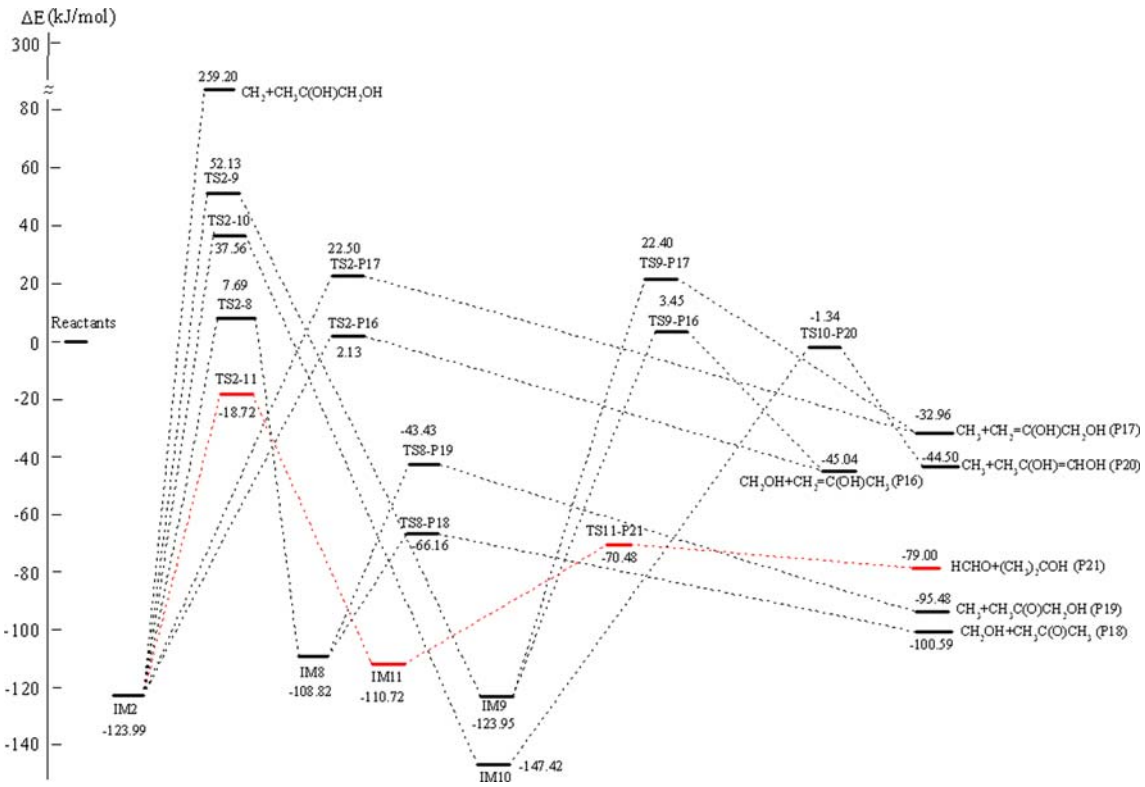

Fig. 6 Profile of the doublet potential energy surface starting from the unimolecular reaction of $CH_2C(OH)$ $(CH_3)CH_2OH$ (IM2) at the CCSD(T)/6-311++G(d,p)//MP2(full)/6-311++G(d,p)+ZPE level. Major pathways are indicated in *red*

The second pathway is that IM1 isomerizes to IM3 via a 1,2-H migration. The corresponding transition state is TS1-3 with a barrier height of 172.49 kJ mol^{-1}. IM3, being 110.01 kJ mol^{-1} below the initial reactants, can decompose to various possible products via three different channels. First, IM3 can undergo a hydrogen loss to produce $C(O)HCH(CH_3)CH_2OH$ (P7) via TS3-P7. Second, the $–CH_2OH$ group loss from IM3 can yield $CH(OH)=CHCH_3$ (P8) via TS3-P8. Third, the $–CH_3$ group elimination from IM3 can lead to $CH(OH)=CHCH_2OH$ (P9) via TS3-P9. These steps face barriers of 148.14, 123.42, and 141.68 kJ mol^{-1}, respectively. The products P8 and P9 are enols. They can proceed further by a 1,3-H shift leading to their corresponding aldehydic structures $C(O)HCH_2CH_3$ (P8A) and $C(O)HCH_2CH_2OH$ (P9A). The corresponding transition states TSP8-P8A and TSP9-9A possess the high barrier heights of 258.83 and 232.03 kJ mol^{-1}, respectively. Therefore, these isomerizations are very unlikely.

The third pathway is that IM1 can undergo 1,3-H-shift to form IM4 via a four-member ring transition state TS1-4 with the relative energy of 133.50 kJ mol^{-1} with respect to IM1. IM4 lies below the reactants by 82.30 kJ mol^{-1}. Two decomposition channels are identified for the intermediate IM4. The first decomposition channel of IM4 is the formation of H+P7 via a C–H bond fission transition state TS4-P7. The second product channel is breaking C–C bond, forming the final products HCHO + CH_3CHCH_2OH(P10) via TS4-P10. The barrier height (58.67 kJ mol^{-1}) for TS4-P10 is 40.42 kJ mol^{-1} lower that for TS4-P7.

The fourth pathway is IM1 isomerization to IM5 by a 1,2-H shift via TS1-5 overcoming a barrier of 176.72 kJ mol^{-1}. IM5 is calculated to be 112.62 kJ mol^{-1} below the initial reactants. It can decompose into CH_2OH + CH_3CH=CHOH (P11), CH_3 + CH_2(OH)CH=CHOH (P12), and H + $CH_2(OH)C(CH_3)$=CHOH (P13) via TS5-P11, TS5-P12, and TS5-P13, respectively. The barrier heights for these conversion transition states are 129.30, 140.99, and 164.02 kJ mol^{-1}.

The fifth pathway is that a hydrogen atom migrates from $–CH_3$ group to the neighboring C atom via a three-center transition state TS1-6. The barrier for such H shift is 170.65 kJ mol^{-1}. This process leads to the formation of IM6, which sits below the initial reactants by 88.96 kJ mol^{-1}. IM6 can decompose into different products such as CH_2OH + CH_2=$CHCH_2OH$ (P14) and H + CH_2=C$(CH_2OH)_2$ (P15) via TS6-P14 and TS6-P15 with barriers of 114.90 and 155.13 kJ mol^{-1}, respectively.

Finally, IM1 isomerizes to form IM7 via a four-center transition state TS1-7, followed by dissociation to yield HCHO+P10 via TS7-P10. The barriers for the isomerization and dissociation reactions are 135.17 and 65.90 kJ mol^{-1}, respectively.

As shown in Fig. 5, IM1 can either dissociate into products H + P6 via TS1-P6, or isomerize to IM2, to IM3, to IM4, to IM5, to IM6, and to IM7 via TS1-2, TS1-3, TS1-4, TS1-5, TS1-6, and TS1-7, respectively. Among the possible reaction channels starting from IM1, the formation of IM2 via a 1,2-OH migration is most favorable. The other channels are not feasible kinetically, for which the corresponding transition states TS1-P6, TS1-3, TS1-4, TS1-5, TS1-6, and TS1-7 lie 36.94, 73.88, 34.89, 78.11, 72.04, and 36.56 kJ mol^{-1} above initial reactants, respectively.

3.3 The unimolecular reactions of IM2

Figure 6 shows the doublet profile of the potential energy surface for the subsequent reactions of IM2. Starting from IM2, many products can be obtained via successive isomerization and dissociation pathways.

IM2 can dissociate into products $CH_2OH + CH_2$=C(OH)CH_3 (P16) and $CH_3 + CH_2$=C(OH) CH_2OH (P17) by breaking the C–C bonds via TS2-P16 and TS2-P17, respectively. The dissociation barriers for TS2-P16 and TS2-P17 are 126.12 and 146.49 kJ mol^{-1}, respectively. The energy of TS2-P16 is only 2.13 kJ mol^{-1} greater than that of the original reactants, so this dissociation channel of IM2 is slightly feasible.

IM2 can also barrierlessly dissociate to $CH_2 + CH_3C(OH)CH_2OH$, which lies above IM2 by 383.19 kJ mol^{-1}. Clearly, this dissociation channels cannot occur to any extent.

IM2 can undergo four different isomerization processes. First, isomerization of IM2 → IM8 occurs by a 1,3-H shift. The corresponding transition state TS2-8 is 131.68 kJ mol^{-1} higher in energy than IM2. Second, IM2 can isomerize to IM9 via a four-member ring transition state TS2-9 with a barrier of 176.12 kJ mol^{-1}. As can be seen in Fig. 6, the value of 176.12 kJ mol^{-1} is the highest barrier for isomerization of IM2. Third, IM2 can transform to IM10 by a 1,3-H migration via TS2-10, which faces a high barrier of 161.55 kJ mol^{-1}. Finally, IM2 can rearrange to IM11 via a five-member ring transition state TS2-11. The barrier for TS2-11 is as high as 105.27 kJ mol^{-1} above IM2, but it is still below the initial reactants OH+MPO221. Summarizing the above four isomerization channels, it can be found that the last isomerization channel faces the lowest barrier. The calculated small barrier indicates that this reaction channel should be efficient.

From the potential energy surface given in Fig. 6, IM8, IM9, IM10, and IM11 lie below the initial reactants by 108.82, 123.95, 147.42, and 110.72 kJ mol^{-1}, respectively. Many decomposition channels of these intermediates would be open.

There are two decomposition channels from IM8 leading to products $CH_2OH + CH_3C(O)CH_3$ (P18) and $CH_3 + CH_3C(O)CH_2OH$ (P19) via TS8-P18 and TS8-P19, respectively. The barriers for the two dissociation reactions are only 42.66 and 65.39 kJ mol^{-1}. Clearly, these dissociation reactions are feasible kinetically if IM8 can be formed.

IM9 can undergo two different dissociation processes. One is the formation of CH_2OH + P16 via a C–C bond rupture transition state TS9-P16, facing a high barrier of 127.40 kJ mol^{-1}. The other is the formation of CH_3 + P17 by breaking C–C bond via TS9-P17 with a 146.35 kJ mol^{-1} barrier. The high barriers indicate that the two dissociation channels are less favorable.

Starting from IM10, there is only one decomposition channel. The decomposition of IM10 can produce $CH_3 + CH_3C(OH)$=CHOH (P20). The transition state for this process is TS10-P20, which has the relative energy of 146.08 kJ mol^{-1} with respect to IM10. Therefore, this channel might play a minor role in the title reaction.

IM11, produced by TS2-11 from IM2, can dissociate to HCHO + $(CH_3)_2COH$ (P21) via TS11-P21 over a 40.24 kJ mol^{-1} barrier. It should be mentioned that the dissociation of IM11 to HCHO + P21 faces the lowest barrier (see Fig. 6). Thus, this step can be expected as the dominant channel.

As can be seen from the discussion above and from Figs. 4, 5, and 6, it is clear that only two low-energy product pathways are expected to be significant: Reactants → PC → TS6 → IM1 → TS1-2 → IM2, and Reactants → PC → TS7 → IM2 → TS2-11 → IM11 → TS11-P21 → HCHO + P21. Accordingly, the predominant products are found to be HCHO+P21 in the title reaction, whereas CH_2OH + P16 are expected to be minor products. Furthermore, the additions of OH radicals to the unsaturated carbon atoms of MPO221 are the rate-determining steps in these reaction channels.

There are no data about the determination of products in OH+MPO221 reaction. Information on the determination of products in the reactions of OH radicals with unsaturated alcohols is only available in the case of CH_2=$CHCH_2$ CH_2OH and CH_3CH_2CH=$CHCH_2CH_2OH$ [6]. Grosjean et al. [6] reported the reaction products of OH with CH_2=$CHCH_2CH_2OH$ in the presence of O_2 and NO. That study demonstrated that formaldehyde and l-hydroxypropanal were formed in the OH-initiated oxidation of CH_2=$CHCH_2CH_2OH$. Formaldehyde was identified as the major carbonyl product. However, l-hydroxypropanal could not be positively identified.

For the analogous reaction of OH with CH_2=C$(CH_3)CH_2OH$, our calculations give the same major product of HCHO in spite of the reaction of OH with MPO221 in the absence of O_2 and NO.

It is interesting to note that the critical points TS6 and TS7 of the rate-determining steps lie 5.19 and 11.14 kJ mol^{-1} below the reactants, respectively. The calculations indicate

that the rate constant of the title reaction should display a negative temperature dependence, and this result is consistent with previous report [2].

4 Conclusion

In the present theoretical study, the complex potential energy surface for the reaction of OH + MPO221 was constructed using CCSD(T)/6-311++G(d,p)//MP2(full)/6-311++G(d,p) level of theory. There are large number of possible product channels including the H-abstraction and the addition–elimination reaction pathways on the doublet potential energy surface. The predicted major products produced from the addition–elimination reactions are HCHO + $(CH_3)_2COH$, while the products CH_2OH + CH_2=C(OH)CH_3 are the minor products with less abundance. The H-abstraction channel OH + MPO221 → P4+H_2O may contribute to the title reaction at higher temperature. The calculated surface indicates that the intermediates and transition states involved in the major product channel are all lower than the reactants in energy, and accordingly, the title reaction should exhibit a negative temperature dependence of its rate constant. This important theoretical result confirms earlier experimental observations.

Acknowledgments This work is supported by the Natural Science Foundation of Xuzhou Normal University (07XLA05). The authors express their gratitude to the referees for their valuable comments.

References

1. König G, Brunda M, Puxbaum H, Hewitt CN, Duckham SC, Rudolph J (1995) Atmos Environ 29:861
2. Cometto PM, Dalmasso PR, Taccone RA, Lane SI, Oussar F, Daële V, Mellouki A, Bras GL (2008) J Phys Chem A 112:4444
3. Guenther AB, Hewitt CN, Erickson D, Fall R, Geron C, Graedel R, Harley P, Klinger L, Lerdau M, Mckay WA, Pierce T, Scholes B, Steinbrecher R, Tallamraju R, Taylor J, Zimmerman P (1995) J Geophys Res 100:8873
4. Imamura T, Iida Y, Obi K, Nagatani I, Nakagawa K, Patroescu-Klotz I, Hatakeyama S (2004) Int J Chem Kinet 36:379
5. Papagni C, Arey J, Atkinson R (2001) Int J Chem Kinet 33:142
6. Grosjean D, Grosjean E, Williams EL II (1993) Environ Sci Technol 27:2478
7. Orlando JJ, Tyndall GS, Ceazan N (2001) J Phys Chem A 105:3564
8. Rudich Y, Talukdar R, Burkholder JB, Ravishankara AR (1995) J Phys Chem 99:12188
9. Hallquist M, Langer S, Ljungström E, Wängberg I (1996) Int J Chem Kinet 28:467
10. Noda J, Nyman G, Langer S (2002) J Phys Chem A106:945
11. Rodriguez D, Rodriguez A, Soto A, Aranda A, Diaz-de-Mera Y, Notario A (2008) J Atmos Chem 59:187
12. Rodriguez A, Rodriguez D, Soto A, Notario A, Aranda A, Diaz-de-Mera Y, Bravo I (2007) Atmos Environ 41:4693
13. Grosjean D, Grosjean E, Williams EL II (1993) Int J Chem Kinet 25:783
14. Grosjean E, Grosjean D (1994) Int J Chem Kinet 26:1185
15. Frisch MJ et al (2004) Gaussian 03, Revision C.02. Gaussian, Inc., Wallingford
16. Møller C, Plesset MS (1934) Phys Rev 46:618
17. Fletcher GD, Rendell AP, Sherwood P (1997) Mol Phys 91:431
18. Hehre WJ, Radom L, Pople JA, Schleyer PR (1987) Ab initio molecular orbital theory. Wiley, New York
19. EMSL Basis Set Library. http://www.emsl.pnl.gov/forms/basisform.html
20. Gonzalez C, Schlegel HB (1989) J Chem Phys 90:2154
21. Gonzalez C, Schlegel HB (1990) J Phys Chem 94:5523
22. Garrett BC, Redmon MJ, Steckler R, Truhlar DG, Baldridge KK, Bartol D, Schmidt MW, Gordon MS (1988) J Phys Chem 92:1476
23. Raghavachari K, Trucks GW, Pople JA, Head-Gordon M (1989) Chem Phys Lett 157:479
24. Werner HJ, Knowles PJ (1985) J Chem Phys 82:5053
25. Knowles PJ, Werner HJ (1985) Chem Phys Lett 115:259
26. Jalbout AF, Boutalib A (2006) J Phys Chem A 110:12524